DEXTRAN-ALLYL ISOCYANATE-ETHYLAMINE HYDROGEL FOR TREATING THIRD-DEGREE DERMAL BURN WOUNDS

By
Hyun Ho (Greco) Song

A thesis submitted to Johns Hopkins University in conformity with the requirements for the degree of Master of Science in Engineering

Baltimore, Maryland
April, 2014

Abstract

Third-degree burn wound is characterized by the full-thickness injury of the skin, including both the epidermal and the dermal layer. These wounds do not heal spontaneously and require excision of the necrotic tissue. Currently, split-thickness skin autografts are commonly used for wound closure, but these can leave thick scars and distorted contractures, which is unfavorable both functionally and aesthetically. In previous works, we have developed a dextran-based hydrogel that is chemically modified with allyl isocycanate and bromoethylamine (Dex-AE) that was tailored to enhance biocompatibility and host-cell infiltration *in vivo*. Polyethyl glycol diacrylate (PEGDA) was added to the hydrogel mix to strengthen the mechanical properties of the hydrogel without compromising the crosslinking density. The therapeutic effect of the gel was first confirmed by the murine *in vivo* burn wound model, where the hydrogel-treated wounds healed completely with regenerated skin appendages by week 8. We then aimed to translate this model into a porcine model because of its structural and biological similarities to the human skin. We first optimized our protocol to create third-degree burn wounds by using different contact temperature and duration. We used this established protocol to conduct our hydrogel treatment studies, where the burned necrotic wounds were first excised and then replaced with our Dex-AE/PEGDA hydrogels. The hydrogel degraded within 5 days after the implantation with higher cell infiltration compared to the control group. In order to analyze the healing process, we have conducted histological assays as well as

blood flow analysis with a speckle contrast imager. Our preliminary data showed signs of higher blood support in the hydrogel-treated wounds that may have contributed to the better epithelial healing that we observed in treated group. We also observed higher cellular infiltration in the areas of the hydrogel-treated wounds compared to the untreated wounds, confirmed by the hematoxylin and eosin staining of the samples at day 2. With additional surgical adjustments, the bioactive hydrogel shows potential for delivering appropriate treatment for third-degree burn wound healing.

Advisor: Dr. Sharon Gerecht

Committee: Dr. Sharon Gerecht and Dr. Denis Wirtz

Acknowledgements

I would like to first thank my parents who have unconditionally supported me throughout my years in the United States to make sure I get the best education possible. They have taught me the value of diligence, self-respect, and independence, and that love is patient and selfless. It has now been a decade since I started living on the opposite side of the earth from them and I miss them very much, but I know that love transcends distance and that it will all worth it in the end.

I would also like to thank Dr. Sharon Gerecht, who has taken me under her wing and given me a tremendous opportunity to explore different aspects of research. I found my passion for translational research during my time in her lab, and her work ethic and dedication to academia inspire me to bring out the best in me. I thank her for believing in me and being the best mentor I could ever asked for. One of my goals is to become a mentor like her.

I would like to thank the members of Gerecht Lab, many of whom have become very close friends of mine over the two years I spent in the lab: Drs. Kyung Min Park and Xin Yi Chan, Sravanti Kusuma, Tom Yu-I Shen, Quinton Smith, Maureen Wanjare, Sebastian Barreto, Kim Ellis, and Matt Davenport. Especially, I would like to thank Tom Yu-I Shen who has equally contributed to this project. I am going to miss our early morning car rides to the animal facility and scholarly conversations about many projects. I also thank Dr. Kyung Min Park for helping me with the materials part of my project and teaching me to

become a better scientist. He also made me appreciate all the resources I have had in my life that I took for granted. I would like to thank Sravanti, Quinton, Xin, Kim, and Matt for being amazing friends and helping me when I was going through the toughest part of my life. I will miss all the positivity that they have brought in my life.

Lastly, I would like to thank Dr. Wirtz for agreeing to be in my committee and witness this very exciting conclusion of my journey at Hopkins.

List of Symbols and Abbreviations

BEAHB	2-Bromoethylamine hydrobromide
AI	Allyl isocyanate
AE	Allyl isocyanate-ethylamine
bFGF	Basic fibroblastic growth factor
CCL2	Chemokine (C-C motif) ligand 2
Dex	Dextran
DBTDL	Dibutyltin dilaurate
DMSO	Dimethyl sulfoxide
W_d	Dry weight of the hydrogel
EGF	Epidermal growth factor
ECM	Extracellular matrix
H&E	Hematoxylin & eosin
HBEGF	Heparin-binding epidermal growth factor
ITGAV	Integrin subunit α-v
ITGB3	Integrin subunit β-3
IL1A	Interleukin-1A
IL1B	Interleukin-1B
MMP	Matrix metalloproteinase
PEGDA	Polyethylene glycol diacrylate
HNMR	Proton nuclear magnetic resonance
qPCR	Quantitative polymerase chain reaction

TEA	Triethylamine
VEGF	Vascular endothelial growth factor
$W_{s,t}$	Weight of the swollen hydrogel at time t

Table of Contents

List of Figures and Tables

Introduction

Burns are a leading cause of accidental death that can result in serious disability and social impairment from disfigurement [1]. In 2013, approximately 450,000 burn injuries received medical treatment [2]. Although the survival rate for burn injuries in general is high, certain categories of burn wounds have higher mortality rates than others. Of these categories, third-degree burn wounds presents the toughest challenge in the clinics. This type of wound is characterized by the full-thickness damage of the skin, including both the epidermal and the dermal layer. Unlike superficial burn wounds that most likely heal on their own without any professional care, third-degree burn wounds do not heal spontaneously and require excision of the necrotic tissue as well as replacement of the wounds with skin substitutes [3].

Wound healing is generally divided into three overlapping phases: inflammation, proliferation, and maturation/remodeling. In the inflammation phase, the transudate is leaked into the interstitial space, where platelets aggregate and form a plug with fibrin [4]. Inflammatory response is characterized by early polymorphonuclear neutrophil infiltration followed by monocyte and macrophage migration [4]. In humans, granulation tissue is formed during the proliferation phase, which occurs within 48 hours of injury [4]. Granulation tissue is a temporarily vascularized connective tissue that is formed by migrating fibroblasts [5]. In this phase, actin-rich myofibroblasts facilitate wound closure by pulling the wound margins together, resulting in wound contraction [4]. Keratinoytes from the epithelium also migrates into the wound to re-epithelialize the wound [4].

Throughout the healing process, Type III collagen is replaced by mature Type I collagen, but the complete remodeling may continue up to 2 years where most amount of change occurs within the first 6 months [4]. However, scarring is inevitable, where the healed tissue can only regain a fraction of the original tissue strength and elasticity [5].

Angiogenesis plays an important role during the proliferative phase of wound healing. During this phase, the vessel capillary sprouts first digest and penetrate the basement membrane and invade the fibrin-rich wound plug to assist migration of other cell types such as fibroblasts and vascularize the granulation tissue [4]. The low oxygen tension in the wounded area creates a hypoxic environment that triggers the vascular endothelial growth factor (VEGF) signaling pathway [6]. Epidermis has shown to produce this factor in large quantities during wound healing to induce angiogenesis, and prolonged angiogenic stimulus by VEGF along with initial stimulus by basic fibroblast growth factor (bFGF) is critical for the neovascularization of the granulation tissue [7, 8]. Existing inflammatory cells at the provisional matrix provide angiogenic cytokines and growth factors as well to facilitate angiogenesis. Transmembrane cell-attachment protein $\alpha_v\beta_3$ has also shown to be essential. Of many integrin receptors that can bind to one or more extracellular matrix (ECM) domains, $\alpha_v\beta_3$ integrin is the only receptor that recognizes fibrin, fibronectin, and vitronectin, which are the characteristic components of a provisional matrix at the wound site [6]. During the invasion of capillaries into the provisional matrix, $\alpha_v\beta_3$ is highly expressed on the migrating vessels, especially at the tips [9]. As the wound ECM composition transitions from fibrin/fibronectin to mature

collagen, most of the new vessels degenerate through apoptosis, and the remaining blood vessels no longer express $\alpha_v\beta_3$ [6].

Some of the characteristics of ideal skin substitute include (i) low cost, (ii) off-the-shelf access, (iii) high flexibility, and (iv) fast vascularization [3]. Split-thickness skin autograft is the current gold standard for wound closure, but it can leave thick scars and distorted contractures, which is unfavorable both functionally and aesthetically. A few synthetic substitutes have made their ways to the market, but most provide only a temporary barrier until autografts are available for permanent closure [10]. Many studies are currently focusing on developing skin substitutes using cells, but there are too many hurdles for these products to go through before reaching the consumer due to strict government restrictions on biological products.

Porcine model has been favored over other animal models for skin wound studies. First, the skin of the pig most closely resembles human skin both anatomically and physiologically. Both have similar dermal-epidermal thickness ratio and dermal vascularization pattern [11, 12]. Biochemically, pig and human skins have similar collagen matrix and keratinous proteins [1]. Studies have also shown an excellent agreement between pig and human with respect to wound healing responses from growth factors such as epidermal growth factor (EGF) and bFGF [12]. In addition, the size of the animal allows control and comparison of different treatment parameters in the same animal, although the total area of wounds often is limited to 10% of the total body surface area. Despite the benefits, not many studies can afford pig model due to its high cost from maintenance, additional personnel, and general drugs administered during the experiment

[1]. In addition, there has been no study that establishes detailed, reproducible burn treatment procedures and wound healing evaluation criteria for large animal models, which further discourages porcine animal studies.

Hydrogels are hydrophilic polymeric networks that are commonly used for creating 3D *in vitro* models of tissues, along with other types of scaffolds, microfluidic devices, and bioreactors. Hydrogels provide means of tuning the mechanical strength and chemical structures of the cellular microenvironment. Studies have shown that different stiffness of gels created by varying crosslinking densities can effect the proliferation, survival, and migration of the embedded cells and can also cue differentiation of stem cells to specific lineages [13-15]. In addition, hydrogels can be chemically modified to present cell-attaching sites (such as RGD amino acid sequence) and matrix metalloproteinase (MMP)-degradable sites which is crucial for tumor progression, endothelial migration, and, ultimately, tumor angiogenesis [15-18]. Over the last few years, our lab has focused on a few design parameters and developed a dextran-based hydrogel called dextran-allyl isocyanate-ethylamine (Dex-AE) that is tailored to promote rapid formation of new functional blood vessels (functional neovascularization) for *in vivo* murine model [19, 20]. The amine groups incorporated in these hydrogels enhance the biocompatibility and integration with the host tissue. In addition, low crosslinking density allows high flexibility of the structure as well as fast infiltration by host cells. Treatment with Dex-AE hydrogel on murine burn wounds with no additional drugs or cells has shown to promote complete skin regeneration with dermal appendages (glands, hair follicles, etc.) by week 5 [20].

Goals

The first goal of this study is to synthesize and characterize the new batches of Dex-AE synthesized to be used for the rest of the study. In addition, we establish surgical protocol for creating third-degree burn wounds on a pig. After we confirm the therapeutic effects of the hydrogel from preliminary *in vivo* murine experiment, the newly synthesized Dex-AE is to be used to investigate its therapeutic effect on a porcine model for third-degree burn wound healing.

Overall Approach

First, newly synthesized Dex-AE is characterized by its mechanical, chemical, and therapeutic properties using swelling analysis, proton nuclear magnetic resonance (HNMR) spectroscopy, and murine burn *in vivo* model. Then, optimal temperature and duration of the contact burn was established to create third-degree burn wounds on a pig. The third-degree damage was confirmed by hematoxylin & eosin (H&E) and Masson's Trichrome staining of the wound histological sections. The wounds created using this protocol was then treated with Dex-AE hydrogels by first excising the necrotic tissue and replacing the excised wound with crosslinked Dex-AE hydrogel (**figure 1**). The healing progress was monitored and evaluated by histological analysis of neovascularization and re-epithelialization, blood flow measurements, quantitative polymerase chain reaction (qPCR), and planimetric analysis.

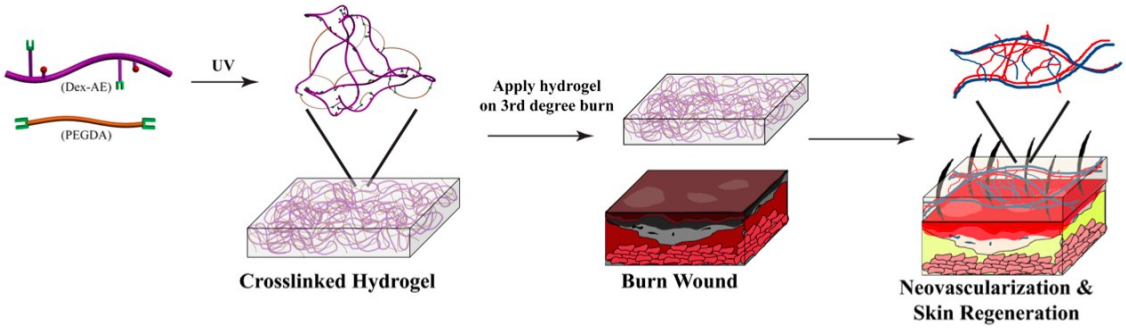

Figure 1. Overall approach. Dex-AE and PEGDA is first crosslinked to form a hydrogel. The burned necrotic tissue is excised and replaced with the crosslinked hydrogel for treatment [21].

Experimental Methods

Materials

Dextran (Dex, MW=70,000), allyl isocyanate (AI), anhydrous dimethyl sulfoxide (DMSO), dibutyltin dilaurate (DBTDL), 2-bromoethylamine hydrobromide (BEAHB), triethylamine (TEA), acryloyl chloride, polyethylene glycol (MW=4,000), deuterium oxide, and other chemicals were purchased from Sigma-Aldrich (St. Louis, MO). Dextran was dried in 60°C overnight before reaction. The photoinitiator Irgacure® 2959 (1-[4-(2-hydroxyethocy)-phenyl]-2-hydroxy-2-methyl-1-propane-1-one) was purchased from BASF Corporation (Florham Park, NJ). Dialysis membrane (MW cut off = 1,000 Da) was purchased from Spectrum Labs, Inc. Male 8-week-old 129S1/SvImJ mice was purchased from The Jackson Laboratory. Yorkshire pigs (~50lb) were purchased from a single breeding farm and were housed and maintained at Thomas D. Morris, Inc. (Reisterstown, MD).

Dextran-Allyl Isocyanate-Ethylamine (Dex-AE) Synthesis

The chemical modification of dextran polymers involved two steps (**figure 2**). First step was the incorporation of AI into dextran. Pre-dried dextran (e.g. 2g) was first dissolved in anhydrous DMSO (20mL) at room temperature under nitrogen gas. Reaction catalyst DBTDL was added (0.210mL), and AI (0.240 mL) was added to the solution dropwise. The reaction was run for 6 hours in 35°C. After the reaction, the solution was precipitated in cold excess isopropanol and filtered. The resulting Dex-AI was then dialysized against distilled water for 3 days and lyophilized for additional 3 days. The purified polymer was stored in vacuum until further use.

The second part of the reaction was the substitution of the remaining hydroxyl groups in Dex-AI with ethylamine groups. For this step, pre-dried Dex-AI (e.g. 2g) was first dissolved in DMSO (30ml) under nitrogen gas. Meanwhile, BEAHB (3.75g) was dissolved in DMSO (10ml) in a separate chamber. Catalyst TEA (11.2mL) was added to the Dex-AI DMSO solution, and the dissolved BEAHB in DMSO was added to the solution dropwise. The reaction was run for 6 hours at 50°C. After the reaction, TEA salt was filtered and the resulting solution was precipitated in cold excess isopropanol and filtered. The resulting Dex-AE was then dialysized against distilled water for 3 days and lyophilized for additional 3 days. The purified polymer was stored in vacuum until further use.

Polyethylene Glycol Diacrylate (PEGDA) Synthesis

PEGDA was synthesized according to previously established method [22]. Briefly, pre-dried PEG (e.g. 8 g) was dissolved in anhydrous benzene under nitrogen gas at 40°C. After complete dissolution, the temperature was cooled down to the room temperature, and TEA (1.19mL) was added. Acryloyl chloride (0.81mL) was added dropwise. The reaction was run for 2 hours at room temperature and then increased to 80°C for an additional hour. TEA salt was filtered after the reaction, and the resulting solution was precipitated in cold excess hexane and filtered. The PEGDA was then dialysized against distilled water for 3 days and lyophilized for additional 3 days. The purified polymer was stored in 4°C until further use.

Preparation of Dex-AE/PEGDA Hydrogel

We dissolved Dex-AE and PEGDA at the weight ratio of 80:20 into phosphate-buffered saline containing 0.1% (w/w) Irgacure® 2959. The mixture was pipetted into a sterile mold made by polydimethylsiloxane (8mm in diameter by 2mm in thickness) and photocrosslinked (10mW/cm^2 of UV light for 10 minutes).

Swelling analysis

The prepared hydrogels were first swollen in distilled water overnight to remove uncrosslinked macromers from the hydrogel. The hydrogels were then dried overnight and the dried weights were measured. The hydrogels were swollen in distilled water, and at specific time points, the wet weights of the hydrogels were measured after the residual

water was removed. The swelling ratio of the hydrogels were calculated by the following formula:

$$Swelling\ Ratio = \frac{W_{s,t} - W_d}{W_d} * 100\%$$

where $W_{s,t}$ is the weight of the swollen hydrogel at time t, and W_d is the dry weight of the hydrogel.

Chemical structure analysis

The newly synthesized Dex-AE polymers were dissolved in deuterium oxide at 10mg/mL concentration. ^{1}HNMR spectroscopy was performed using AMX-300 NMR spectrometer (Bruker) at 300MHz frequency. The reference peak was set at 4.8ppm.

Murine surgery procedure

Surgical procedures were approved by the Johns Hopkins University Animal Care and Use Committee and are reported previously in detail [21, 23]. Briefly, the burn injury was created with a 220g aluminum rod (1.2cm diameter) heated in a 100°C water bath for 5 min. The wounds were created on the posterior-dorsum of each mouse for 4 seconds. The necrotic skin was removed full-thickness with an 8mm diameter biopsy punch. The wounds were then treated with the hydrogels and covered with DuoDerm dressing (ConvaTec Co.).

Porcine surgery procedure

Surgical procedures were approved by the Institutional Animal Care and Use Committee at Thomas D. Morris, Inc. prior to the experiments. All pigs were fasted for at least 12 hours prior to any surgical procedure. Anasthesia was induced by an intramuscular injection of Telazol cocktail reconstituted with ketamine and xylazine. Then, the pig was endotracheally intubated and ventilated mechanically to aid breathing and to provide up to 1.5% of isoflurane (depending on the painfulness of the procedure) to maintain anasthesia. In addition, blood pressure, heart rate, body temperature, and blood oxygen level was monitored. Bair Hugger® was placed under the pig and set to 43°C to maintain a normal body temperature.

Thoracic paravertebral zone was chosen as the burn site to minimize the trauma resulting from pig's movement or lying. Before creating the wounds, the hair at the burn site was removed with a razor blade followed by the sterilization of the area with iodine.

Two parameters were optimized to establish third-degree burn wound protocol via a separate live-pig study: duration of the contact burn and the temperature of the metal bar. The metal bar was first heated using a heating plate (Fisher Scientific, Inc.) to 100°C or 200°C, monitored with the thermometer. The device was aligned perpendicular to the skin's surface and applied for 15, 30, or 60 seconds at a constant pressure of 2kg/cm^2. Histological sections were obtained at day 1 and day 2 to assess the degree of burn damage.

Two pigs were used to investigate the therapeutic effect of Dex-AE hydrogel on burn wounds. The wounds were left alone for 48 hours for stabilization before the

excision procedure. In the first pig, a total of 22 circular third-degree burn wounds (1.5cm in diameter) were created. A circular biopsy punch with a diameter of 1.2cm was used to excise out the full-thickness wound down to the necrotic adipose layer. Peripheral wound was left unexcised to simulate a clinical practice [20]. In the second pig, a total of 20 burns wounds were created (4 bigger square wounds with sides of 3cm, 16 smaller circular wounds with diameters of 1.5cm). Wounds were at least 3cm apart from one another to minimize hindered wound healing process due to one another. Bigger wounds were excised to completely remove the necrotic tissue, and the smaller wounds were excised the same way as the first pig.

After the excision procedure, wounds were cleaned with sterile gauze to temporarily stop bleeding. Half of the wounds were treated with Dex-AE hydrogel and the other half were left untreated. Hydrogels were crosslinked with sizes that matched the size of the excised wounds. Treated and untreated wounds were first sealed with Tegaderm® (3M). The peripheries of the wound site was applied with compound benzoin tincture (Medical Chemical, Corp) to enhance the Tegaderm® adherence to the skin. VetRap® (3M) was wrapped around the dorsal and the ventral areas to keep the first layer in place. Finally, a body suit (VetMedCare) was worn over the body. After the hydrogel was degraded, all wounds were placed with a non-adhesive, non-absorptive dressing Curity™ (Covidian) to prevent epidermal damage when removing Tegaderm® (**figure 2**).

Dressings were changed three times a week until wound closure was complete. Before the dress change, the pig was put under anesthesia with an intramuscular injection of Telazol cocktail reconstituted with ketamine and xylazine. The pig did not receive

isoflurane because the procedure was quick. Before reapplying dressings, the wound area was scrubbed with 4% chlorhexidine and ethanol. The area was wiped with dry gauze and new dressings were applied.

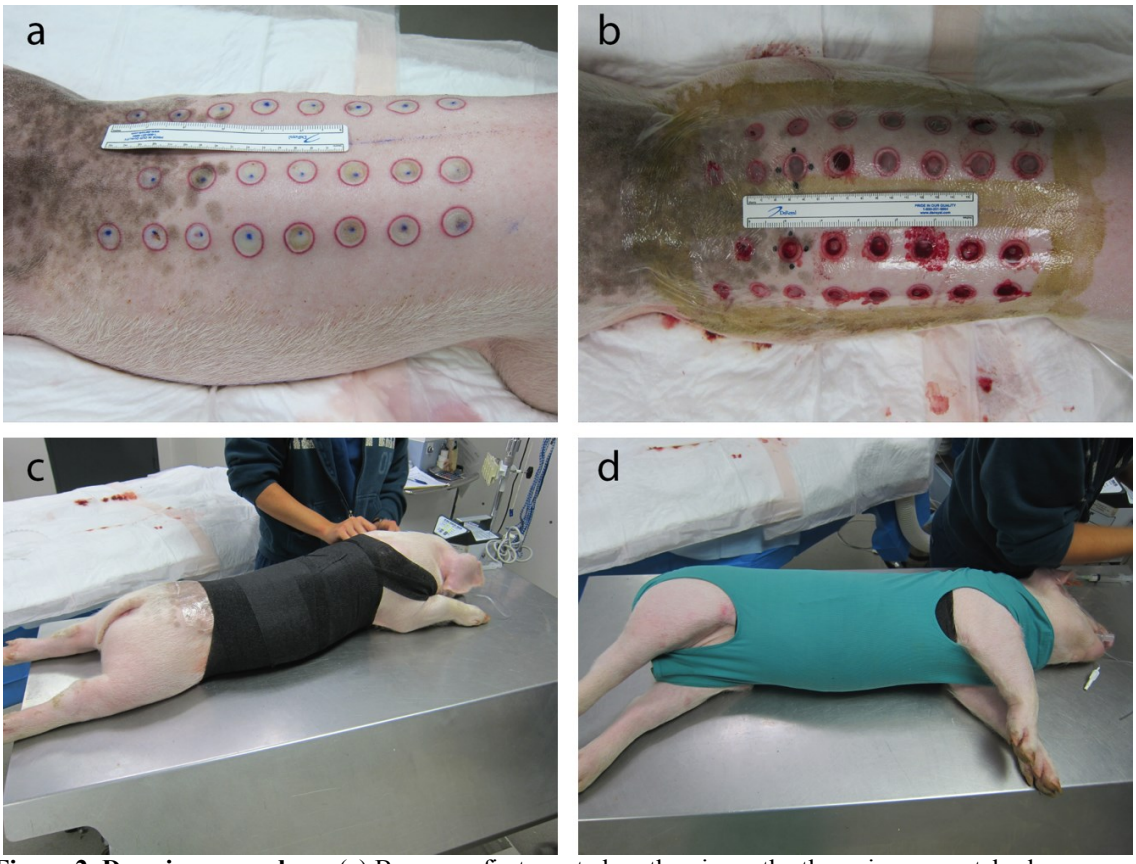

Figure 2. Dressing procedure. (a) Burn was first created on the pig on the thoracic paravertebral zone. After the excision, the treated group received hydrogels inside the excised area and the non-treated group wounds were left excised. (b) The peripheries of the thoracic paravertebral zone were coated with benzoin, and the wounds were dressed with Tegaderm®. (c) The subject was then wrapped with VetRap®. (d) A body suit was put over the body.

To evaluate healing, skin specimens were biopsied at each time point as complete horizontal cross-sections of approximately 5cm in thickness with a sterile blade.

Analgesics was administered before wound creating and biopsy procedures, and transdermal fentanyl patch was applied for 9 days post-operation.

Blood test was performed regularly to monitor the pig's health throughout the study.

Evaluation of Wound Healing

During the study, the blood flow inside the wounds were monitored noninvasively using moorFLPI speckle contrast imager (Moor Instruments, Inc.). The measurement was normalized by the blood flow measurement of the healthy skin area adjacent to each wound.

For immunohistochemical assay, collected skin specimens were first fixed with 10% formalin (Fisher Scientific, Inc.) for at least 48 hours. Following fixation, samples were dehydrated in graded ethanol (70% to 100%), embedded in paraffin, sectioned at 5 μm, and stained with either H&E or immunohistochemistry for CD31 (Abcam, Dako), α-SMA (Dako), cytokeratin 14 (Abcam), and Masson's trichrome.

The area and number of vessels inside the wounds were quantified using ImageJ software (National Institutes of Health) with histology sample of each wound stained with CD31. The vessels were imaged at the edges, middle, and top portions of each wound, and the positively stained areas were selected using the software's threshold function. The selected areas were then quantified using "Analyze Particles" plugin of ImageJ. "Vessels" with areas less than $78\mu m^2$ were excluded to filter out noise.

Epithelial thickness was visualized with the immunohistochemical staining of cytokeratine 14 and was quantified using ImageJ. For each wound, at least 12 thickness measurements were made and averaged to calculate the average distance between the surface and the basement membrane of the epithelium.

Two-step reverse transcription polymerase chain reaction (qPCR) was performed on wound specimens in accordance with Applied Biosystems manufacturer instructions [24]. To extract RNA, a small specimen was collected from each wound at different time points and snap-frozen in liquid nitrogen. The specimen was crushed with pestle and mortar, and the powdered sample was put in 1mL of Trizol reagent and stored in -80°C until further use. Wound healing PCR array sets were purchased from Qiagen to compare the expression profile inside the treated and non-treated wounds at different time points. For each primer, the comparative computerized method provided by Qiagen was used to calculate the amplification differences between different samples.

Statistical analysis

Statistical analysis was performed with either one-way ANOVA with Tukey's post tests or two-way ANOVA with Bonferroni post tests where appropriate using GraphPad Prism® 6. Significance levels between the non-treated wounds and treated wounds were set at: $*p < 0.05$, $**p < 0.01$, and $***p < 0.001$.

Two wounds per condition were created on a porcine cadaver for optimizing the surgical procedure to create 3rd degree burn wounds. For the subsequent hydrogel studies, at least two wounds were created per time point for biopsy.

Results

Dex-AE /PEGDA Hydrogel Preparation

Dextran was first functionalized with acrylate group to facilitate crosslinking reaction via photocrosslinking reaction under a long wave ultraviolet lamp. The overall schematics of the reaction is shown in **figure 3**. During the reaction, a fraction of hydroxyl group reacts with the isocyanate (NCO-) group of AI via nucleophilic attack, resulting in urethane bonds. ^{1}HNMR spectroscopy revealed the degree of substitution of AI to be 0.25 (**figure 4**). The hydroxyl groups in Dex-AI that have not been functionalized with AI were reacted with BEAHB. Amine group is a weak base that readily ionize, and even when not ionized, the high electronegativity of nitrogen result in partial charge that make it highly hydrophilic. In addition, amine-functionalization in hydrogels has shown to enhance biocompatibility and drug release profile [19]. ^{1}HNMR spectroscopy revealed the degree of substitution of AI to be 0.05.

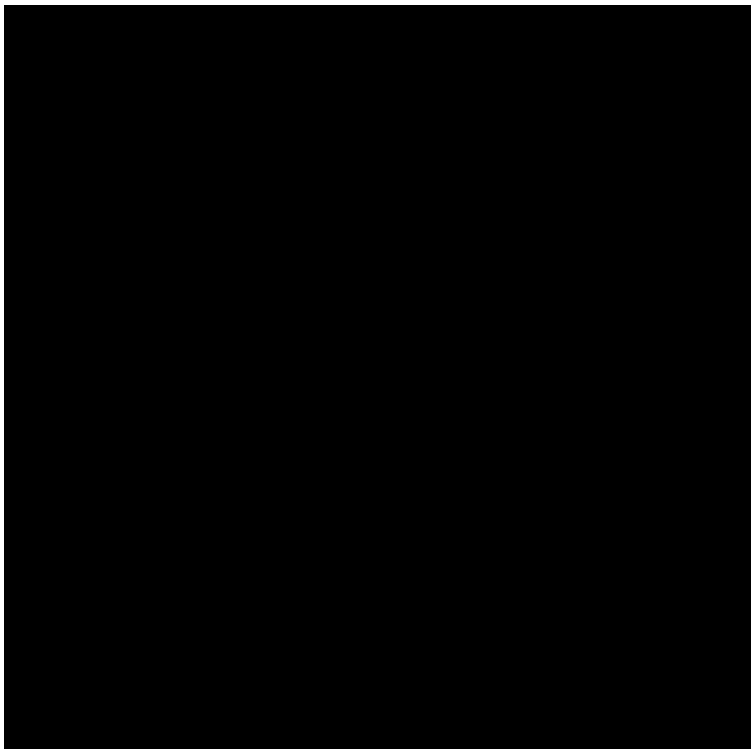

Figure 3. Chemical modification of Dex-AE. The hydroxyl groups in dextran were first modified with AI and further modified with BEAHB to form Dex-AE.

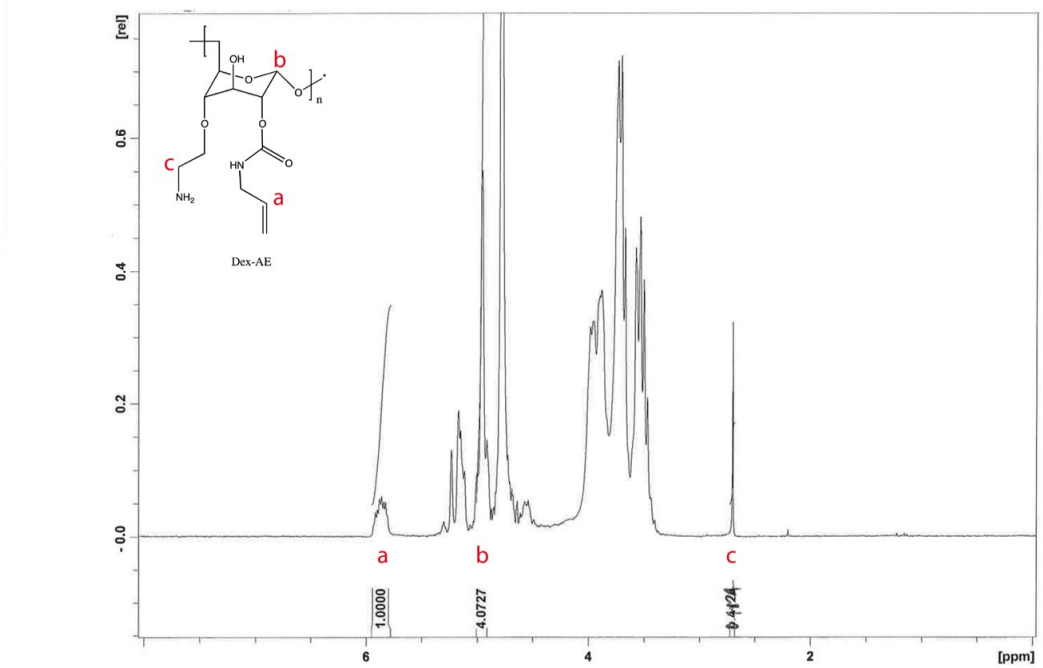

Figure 4. ^{1}HNMR spectroscopy of Dex-AE. Spectroscopy data showed 0.25 allyl DS and 0.05 amine DS.

Although low DS value of acrylate group allows low crosslinking density and high hydrogel pore size that facilitates host cell infiltration, Dex-AE hydrogel is unstable and does not have enough structural durability to retain a three-dimensional shape. PEGDA was added to the polymer mix to provide mechanical strength. Previous study has shown that mixing Dex-AE with PEGDA in the ratio of 80/20 allows mechanically durable hydrogel (elastic modulus of ~1kPa) without compromising the loose interior architecture [20]. PEG is not biodegradable, but low molecular weight PEG polymers are readily excreted from the body are already approved by the FDA for medical uses. extensively for a drug delivery, stem cell differentiation, and cell-patterning [25]. PEGDA is innately hydrophilic, and the Dex-AE/PEGDA hydrogel is able to retain water up to 3,500% of its dry weight (**figure 6**). This makes the hydrogel a great candidate for skin scaffold since the ability to maintain hydration is critical for the healing of burn wounds [4].

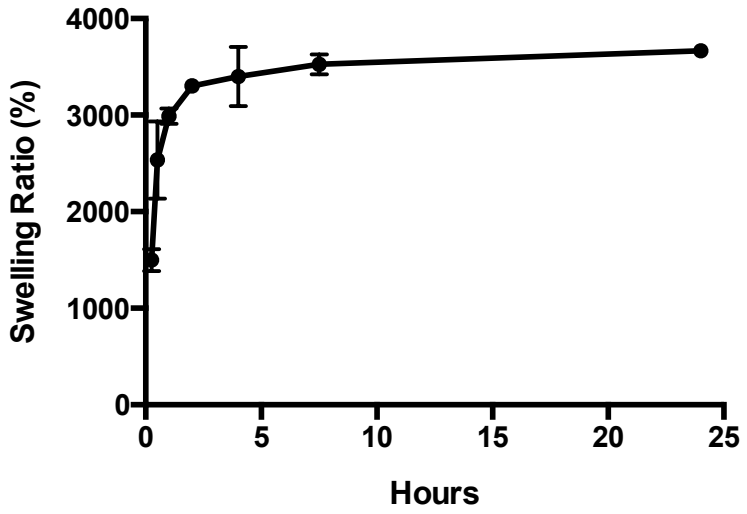

Figure 5. Swelling kinetics of Dex-AE/PEGDA hydrogel.

Treatment of burn wounds with Dex-AE/PEGDA hydrogels on mice

In order to investigate the therapeutic effect of Dex-AE/PEGDA hydrogel on burn wounds, necrotic burn wounds were excised and treated with the hydrogels for 8 weeks. H&E staining of week 3 biopsy samples of treated wounds showed complete re-epithelialization of the wounds (**figure 7a**). Complex structures that resemble skin appendages were also observed at week 3, and by week 8, skin was fully healed with hair growth (**figure 7b**). Previous report has shown high inflammatory and angiogenic cell infiltration in hydrogel-treated wounds, expediting and aiding the wound healing process [21].

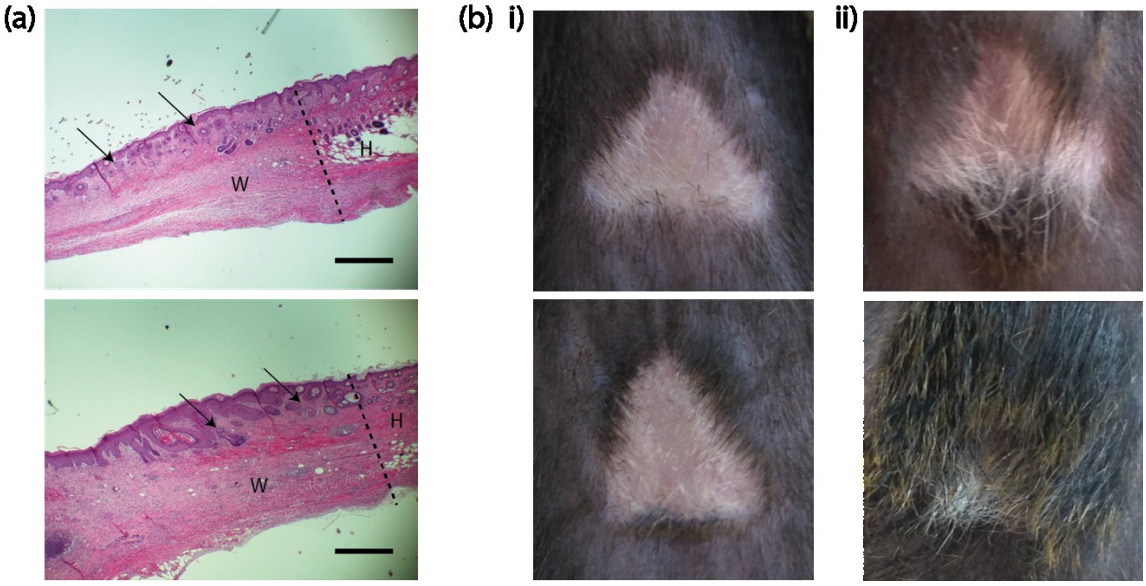

Figure 6. Treatement of murine burn wounds with Dex-AE/PEGDA hydrogel. (a) H&E staining of wound samples from two different hydrogel batches at day 7. Arrow shows the formation of glands. W = healing wound, H = healthy skin. (Bar = 500μm) (b) Macroscopic view of the healing wounds treated with the hydrogels at i) week 5 and ii) week 8.

Creation of third-degree burn wounds on pigs

Pig is a great model for wound healing studies for the reasons explained in the introduction. However, an appropriate protocol for creating burn wounds in a third-degree level must first be established. **Figure 7** shows the custom-made device for creating burn wounds [26]. The device is comprised of three parts. The metal rod part is made of stainless steel which is used for contact burn once it is heated up. The middle part is an insulating unit made of polytetrafluoroethylene for holding the device upright for the duration of the burn. The syringe part provides a spring force from the trapped air, which can be kept consistent for all wounds by applying the same amount of pressure using the side measurement marks. The metal rod part was designed to be exchangeable to be able to minimize the time needed to heat the metal by using multiple rods. In addition, each rod was drilled with a small hole to monitor its core temperature with a digital thermometer (ThermoFisher Scientific, Inc.). Two critical parameters for burn wounds are temperature of the burning object and the duration of the contact with the object [5]. Pressure can also affect the degree of the burn damage, but not as much as temperature and the duration [27]. Therefore, an appropriate value of pressure was simply chosen and kept constant for the entire study at $2kg/cm^2$.

Figure 7. Burn wound device. The stainless steel unit was custom-made to create the desired wound size. The syringe part provides a measureable and controllable compressive force when creating the burn. The insulating unit was placed to hold the device in the upright.

The degree of burn damage was evaluated by H&E and Masson's Trichrome stains of wounds 24 hours or 48 hours after the burn (**figure 8**). Tissue damage from burn is characterized by (1) purple H&E staining of the area and (2) red Trichrome staining of the area which represents damaged collagen [26, 28]. Of all the parameters we tested, damage in collagen was only observed in wounds burned at 200°C. In addition, the damage seemed to progress between 24h and 48h for this temperature. For significant burn damages, a progression of burn depth can be found until 48h post-injury compared to superficial damages [29]. For duration, both 30 seconds and 60 seconds at 200°C yielded wounds with third-degree damages after 48 hours, but 30 second contact yielded more consistent results compared to 60 seconds with less error. In addition, 60 second contact with the heated object created a much bigger wound compared to 30 second contact due to the longer exposure to the peripheral heat from the stainless steel rod. Therefore, optimal parameters (200°C for 30 seconds) were chosen and used for the rest of the study to create third-degree wounds.

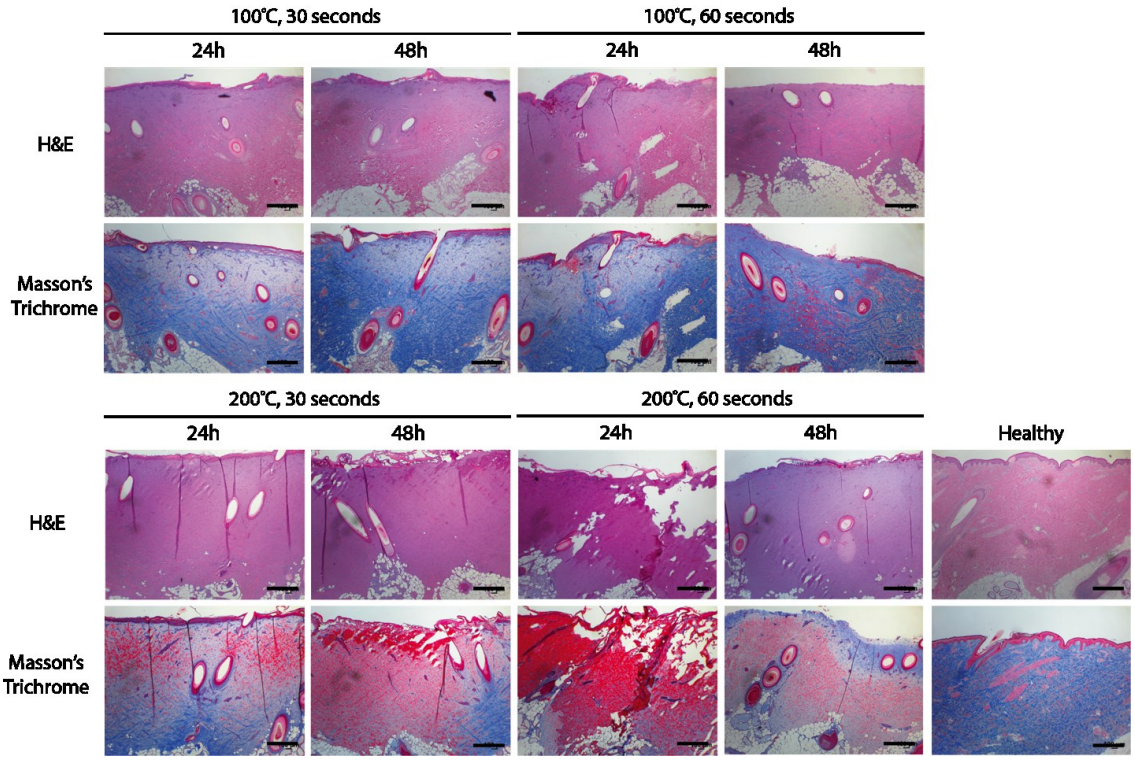

Figure 8. Extent of burn injury of porcine skin using different contact temperature and duration.

Treatment of burn wounds with Dex-AE/PEGDA hydrogels on pigs

In the first hydrogel study, we created a total of 22 third degree burns with 1.2cm diameter stainless steel device (**Figure 9**). The resulting wounds were bigger than the diameter of the heated device (about 1.5cm diameter) due to the damage from the peripheral heat. A biopsy punch with a diameter of 1.2cm was used to excise out the wound, leaving out some peripherally damaged tissue to simulate a method practiced on humans in some clinics [21]. **Figure 10** shows the histological staining of CD31 and α-SMA from the first hydrogel study. CD31 is a characteristic marker for blood vessel endothelial cells. α-SMA stains the smooth muscle actins found in smooth muscle cells that surrounds blood vessels as well as those found in myofibroblasts that are responsible

for the contraction of the wounds. Most myofibroblasts were found at the edges for both treated and non-treated group. However, we observed much stronger myofibroblast stains for non-treated group compared to the treated group. Quantification of vessels stained with CD31 showed similar average vessel area and vessel density for both non-treated and treated groups except for the top part of the wound for week 1 (**figure 11a**). On week 1, the vessels grown in the hydrogel treated wound were significantly larger than those in the non-treated wounds. The quantification generally agrees with the blood flow measurements taken with the speckle contrast imager, although the histological analysis was done less frequently compared to blood flow measurements, resulting in missing the time point when the blood flow hit the maximum (**figure 11b**). Overall, both non-treated and treated group showed a pattern of increasing blood flow in the early time points (day 0 to day 12) followed by regression.

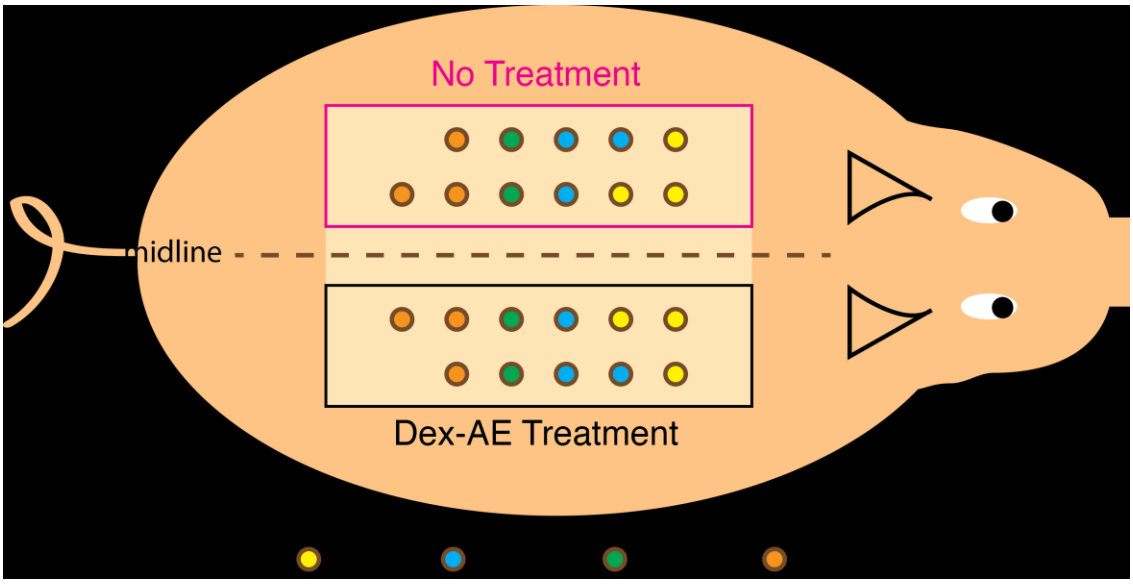

Figure 9. Wound schematic of the first porcine hydrogel treatment study. Each wound was created with a 1.5 cm diameter, and after 48 hours, 1.2 cm diameter of the necrotic tissue was excised out, leaving a thin rim of necrotic skin.

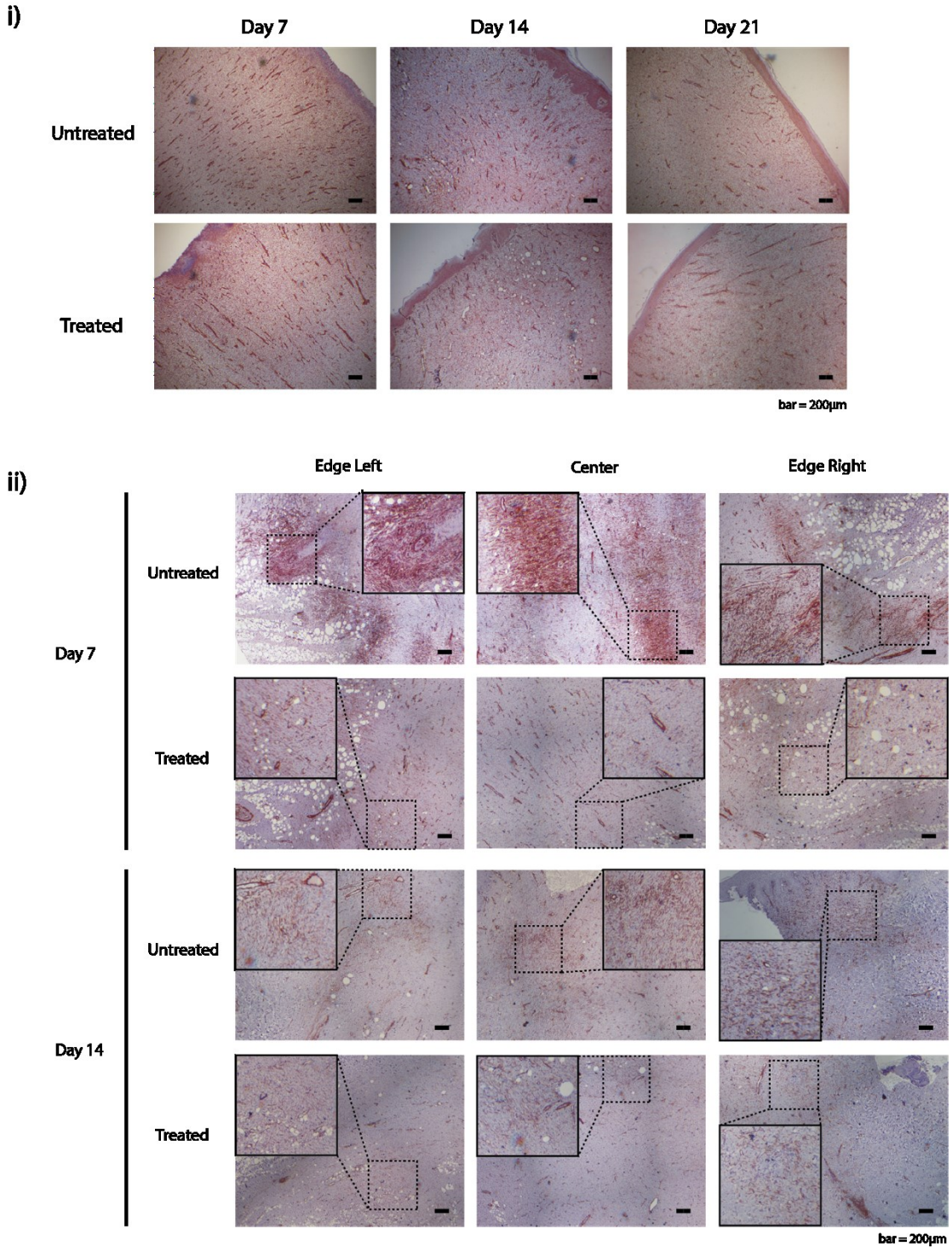

Figure 10. Vascular and myofibroblast characteristics in healing wounds. (a) CD31 staining of wounds at days 7, 14, and 21. (b) α-SMA staining at days 7 and 14 of different areas of the wounds.

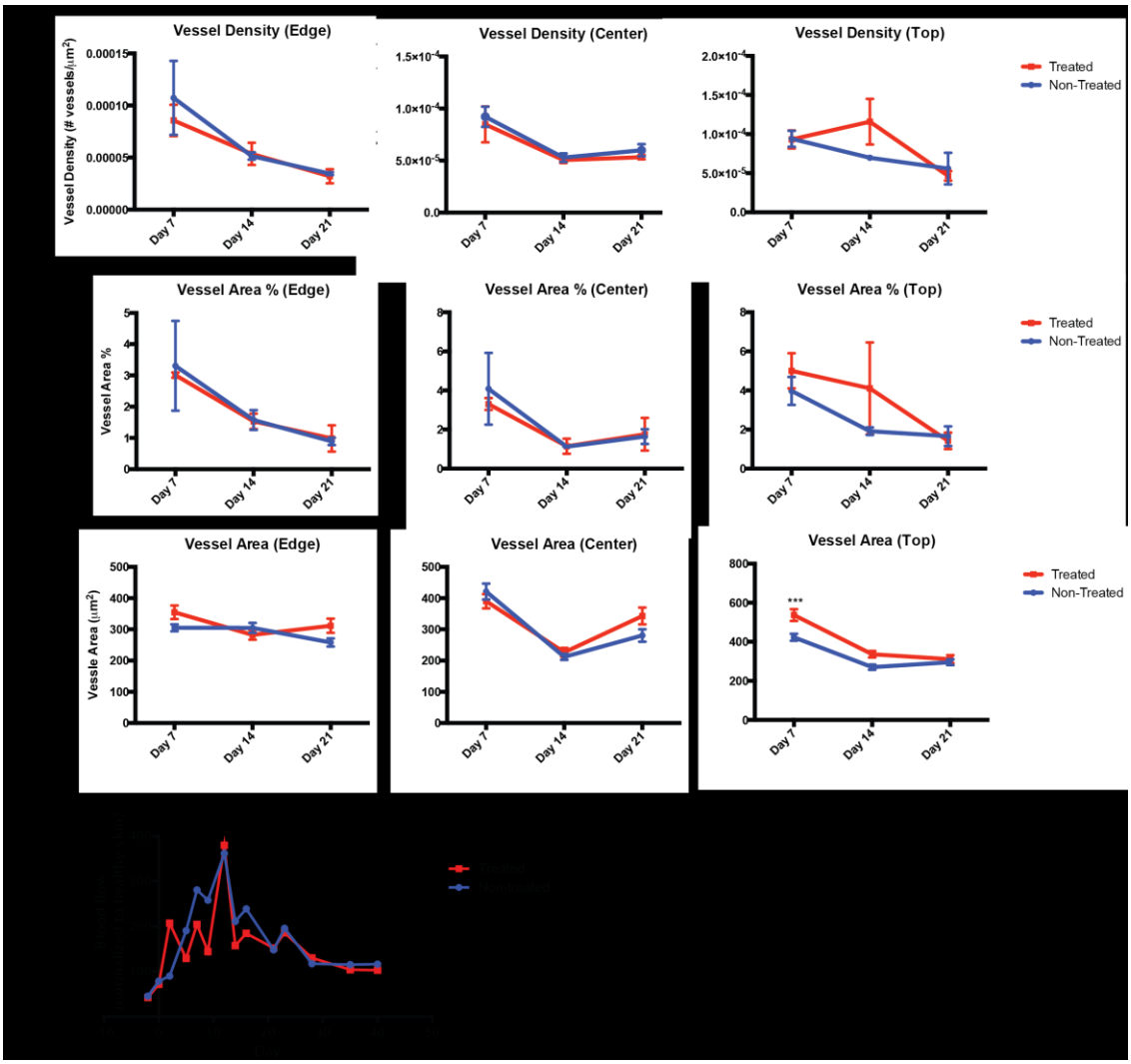

Figure 11. Quantification of vascular characteristics of healing wounds. (a) Quantification of i) vessel density, ii) area % covered by the vessels, and iii) the average are of the vessels from the histological samples of healing wounds at days 7, 14, and 21. (b) Blood flow measurements from speckle contrast imager up to day 40. Day -2 is the time point when the burn wound was created.

Re-epithelialization was completed in about 14 days for both non-treated and treated wounds. Cytokeratin 14 (K14) stain of wound histology samples showed the thinning of the epithelium layer after the re-epithelialzation was completed (**figure 12a**). Treated wounds' epithelium layers thinned to the thickness comparable to the healthy skin (**figure 12b**).

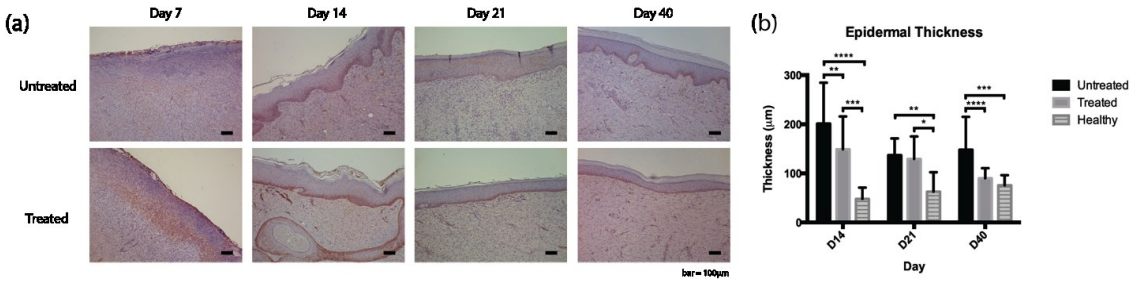

Figure 12. Epidermal characteristics of healing wounds. (a) K14 staining of healing epithelium at days 7, 14, 21, and 40. (b) Quantification of epidermal thickness at days 14, 21, and 40.

The first pig was monitored for 40 days after the treatment of the wounds. **Figure 13** shows the macroscopic representation of the healing process for the treated and non-treated wounds. Macroscopically, the treated and non-treated wounds did not look very different from one another.

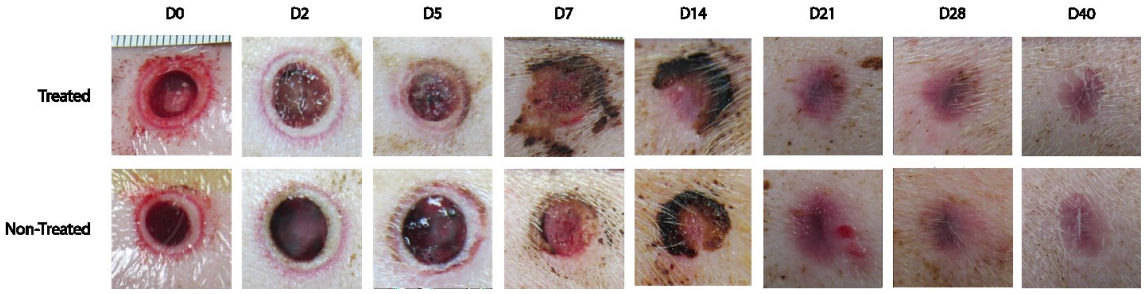

Figure 13. Macroscopic view of the healing wounds.

From the first hydrogel study, we learned that the hydrogel degraded completely within a week, and we needed to further characterize the wound kinetics within the first week of healing process at the histological level. In addition, not a lot of differences between the treated and the non-treated were observed, and we suspected that either the

peripheral burn wounds that were left out from being excised were screening the therapeutic properties of the hydrogel or the wounds were too small that body's own spontaneous healing mechanism is good enough that the hydrogel did not help. With the second study, three issues were investigated: (1) the host-material interaction between Dex-AE/PEGDA hydrogel and the skin at earlier time points (< d7), (2) change in healing kinetics by the complete excision of burned necrotic tissue before hydrogel treatment, and (3) the therapeutic effect of the hydrogel on a bigger wound. In order to address this, we created 4 bigger wounds (3cm x 3cm) and 16 smaller wounds (same size as those in first hydrogel study). For the bigger wound, square shape was chosen to visualize contraction better and to be able to collect smaller circular biopsy samples (0.6 cm diameter) at multiple time points from the same wound. **Figure 14** shows the schematics of the wound for this second study. The smaller wounds were excised and treated the same way as they were in the first study, where some of the peripheral burn wound was not excised. The bigger wounds were completely excised including the peripheral burn wound. One bigger wound in each group was tattooed around the edges to monitor wound contraction throughout the study. The healing process was monitored for 60 days.

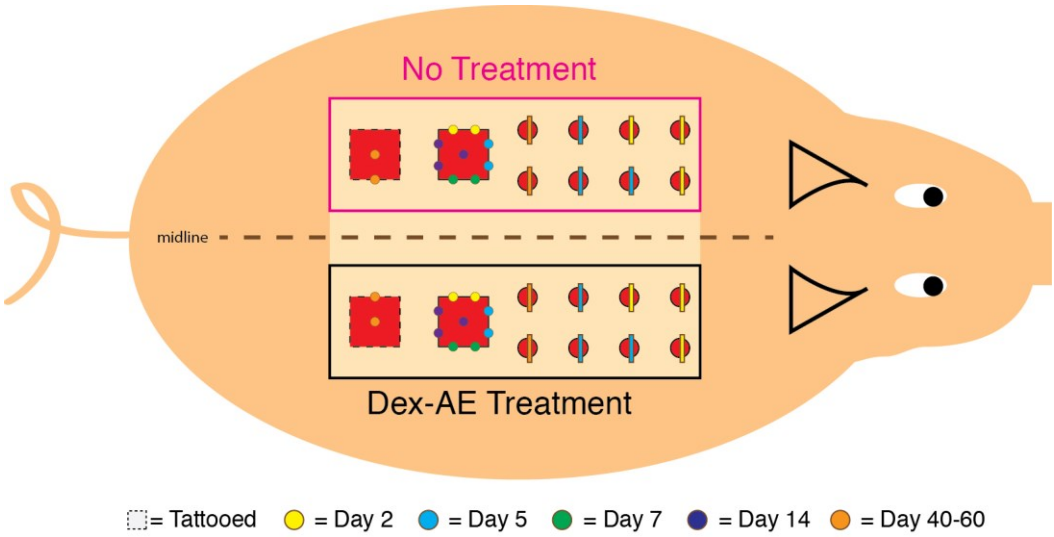

Figure 14. Schematics of the wounds created on the second pig. Each smaller wound was 1.5 cm in diameter, and 1.2 cm of its necrotic tissue was excised out, leaving some peripheral wound at the rim. Each bigger wound was a 3 cm by 3 cm square, and all of its necrotic tissue was excised out.

Dex-AE/PEGDA hydrogel is degraded by the host cells within five days after the hydrogel implantation. Hydrogel was observed in histological sample with some cellular ingrowth in day 2 (**figure 15**). However, No vessels were observed inside the wound yet. In day 5, newly formed vessels were observed at the edge, but had not yet reached the center of the wound (**figure 16a**). The quantification of vessels showed that at the edges, more area was covered by the vessels in the treated wounds compared to the non-treated wounds (**figure 16b**). This was also confirmed by the speckle contrast imager blood flow data at the edges (**figure 16c**). Macroscopically, the small wounds did not show significant differences between treated and untreated groups, similar to the first hydrogel study (**figure 17**).

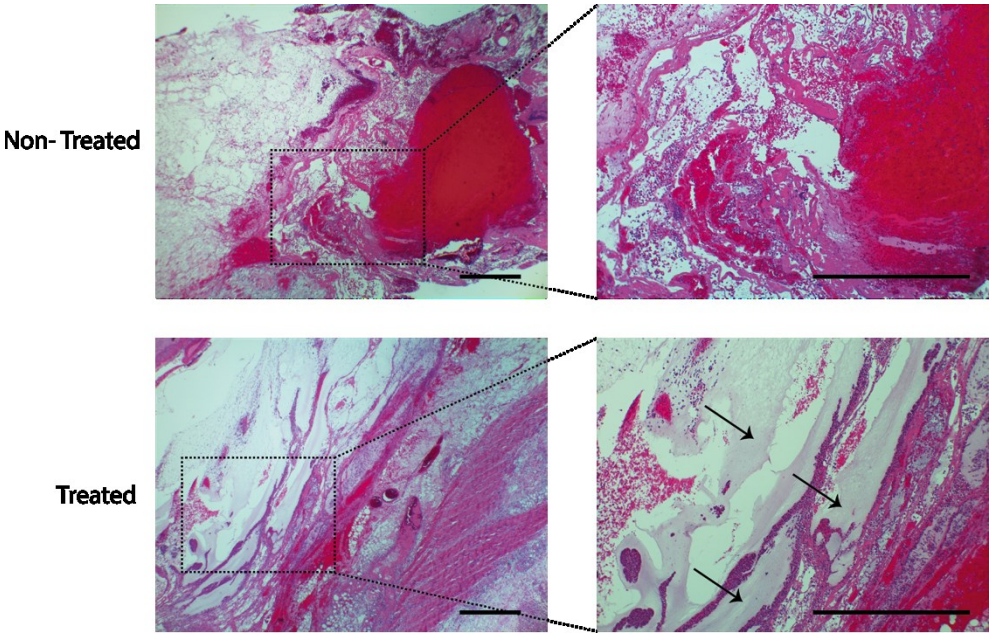

Figure 15. H&E staining of healing wounds at day 2. Arrow heads point to hydrogel fragments that have not been degraded. (Bar = 500µm)

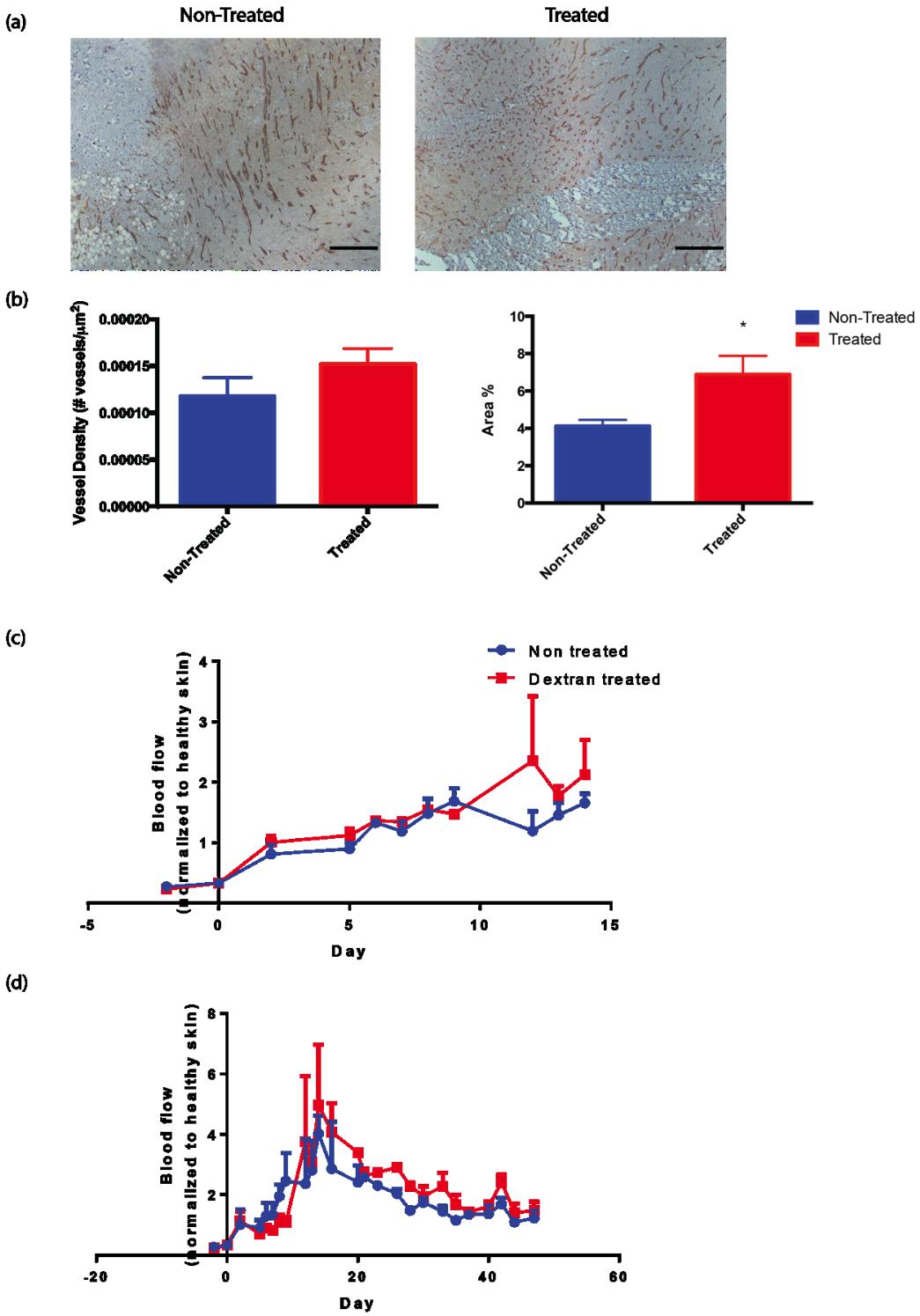

Figure 16. Vascular characteristics of the healing wound at day 5. (a) CD31 staining of the wound histology sampels. (Bar = 500μm) (b) Quantification of vessel density and the area covered by the vessels at the edge of the healing wound at day 5. (c) Blood flow measurements of the wound edge areas at early time points. (d) Blood flow measurements of the total wound areas up to day 56.

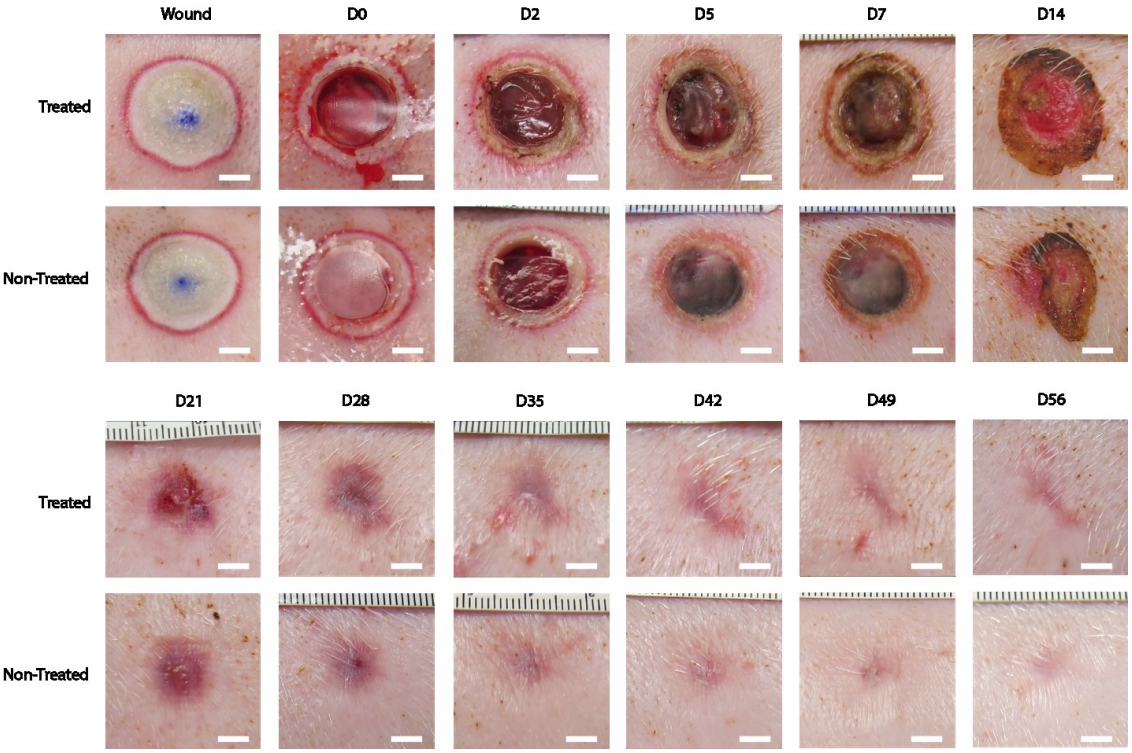

Figure 17. Macroscopic view of the wound healing progression. (Bar = 5mm)

Full excision of the peripheral wounds seems to increase cell infiltration and enhance the host-material interaction. H&E staining of the wound edges at day 2 showed much more cells infiltrated inside the hydrogel compared to the non-treated wound (**figure 18**). In addition, there seems to be a difference between treated and non-treated wounds in on day 7 at the edges in terms of the area covered by the new vessels and the number of vessels per area, although more data is needed to check statistical significance (**figure 19a&b**). Speckle contrast imaging measurements of blood flow revealed slower healing kinetics of bigger wounds compared to the small wounds, evaluated by delayed regression of flow (**figure 19c**). In addition, a couple of spikes in blood flow were observed for wounds from both groups whenever the subject scratched its back and disrupted the healing epithelial layer.

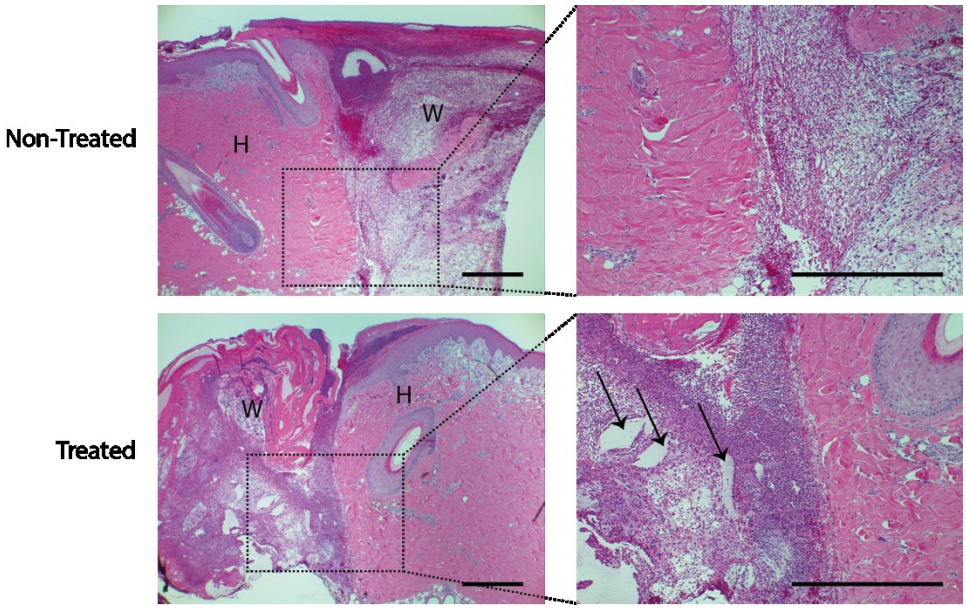

Figure 18. H&E staining of edges of bigger wounds (3cm x 3cm) at day 2. Arrow heads point to hydrogel fragments that have not yet been degraded. W = healing wound, H = healthy skin. (Bar = 500µm)

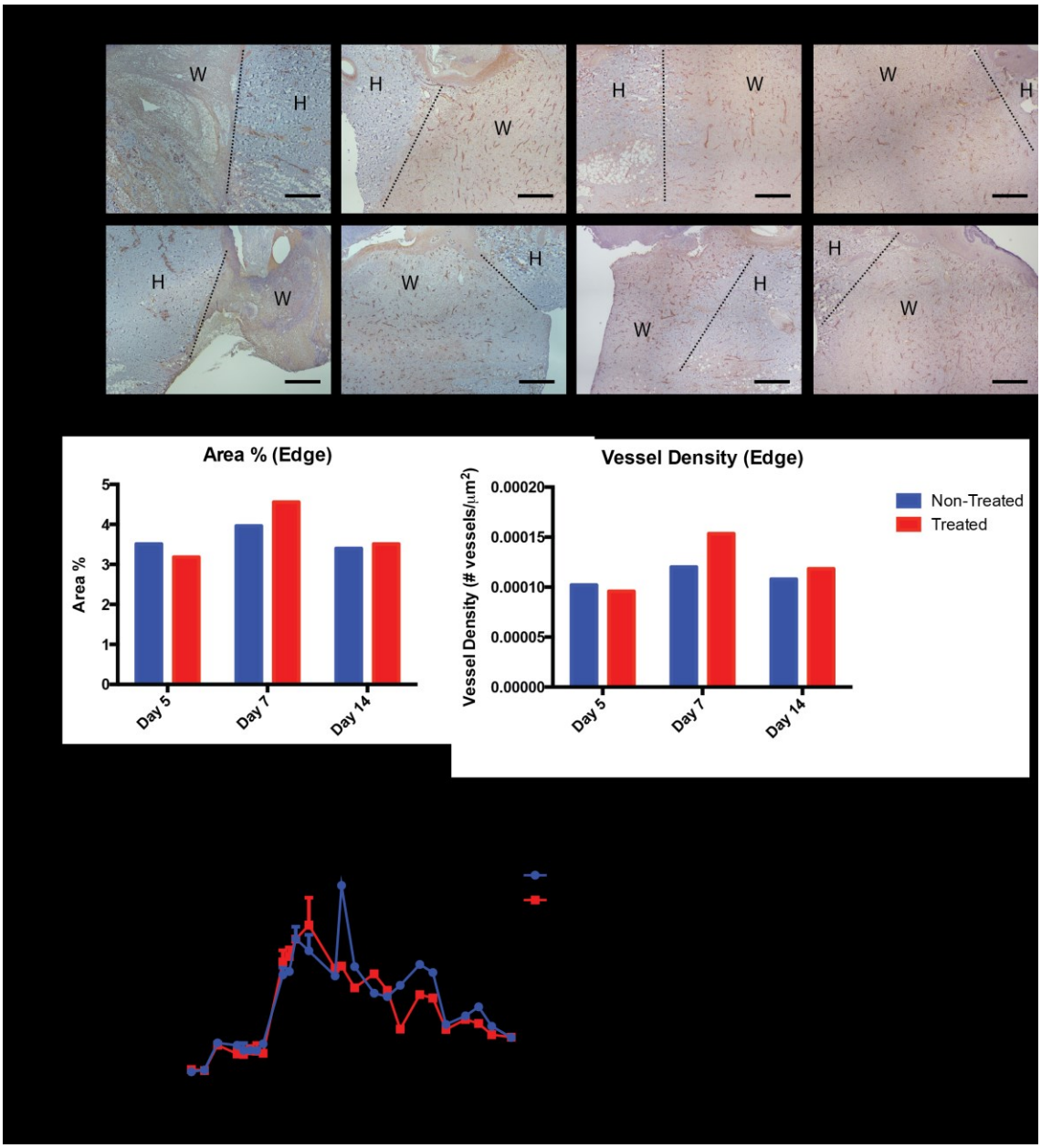

Figure 19. Vascular characteristics of healing bigger wounds (3cm x 3cm). (a) CD31 staining at the edges of the wounds. W = healing wound, H = healthy skin. (Bar = 500μm) (b) Quantification of the area covered by the vessels and the vessel density at the edges of the wounds. (c) Blood flow measurements from speckle contrast imager of the wounds.

Performing qPCR on day 14 large wound samples revealed key differences in gene expression profiles between treated and non-treated groups (**Table 1**). Notably, almost three-fold higher expression of integrin subunit β_3 (ITGB3) was observed in the treated wound compared to the non-treated wound. When dimerized with integrin subunit α_v (ITGAV), integrin β_3 aids in endothelial cell migration into the provisional matrix [6]. Almost two-fold higher expression was observed for MMP-9 in treated wound. MMP-9 aids keratinocyte migration and granulation tissue remodeling [30, 31]. In contrast, MMP-3 expression was lower in treated wound by 0.5 fold. We also observed lower expression of inflammatory cytokines IL-1A and -1B and chemokine (C-C motif) ligand 2 (CCL2) in treated wound by less than 0.5 fold. Heparin-binding epidermal growth factor (HPEGF), which is known to enhance stromal cell recruitment, re-epithelialization and angiogenesis, was also expressed lower than the non-treated group by 0.4 fold [32, 33].

Genes	Fold Change (treated/non-treated)
HBEGF	0.4241
CCL2	0.4715
IL1A	0.4447
IL1B	0.2667
ITGAV	1.0837
ITGB3	2.7552
MMP3	0.4562
MMP9	1.7001

Table 1. Expression of key wound healing genes at the wounds at day 14.

Macroscopically, wounds from both groups appeared similar in terms of discoloration and re-epithelialization (**figure 20a**). Quantification of the area also revealed similar contraction trend between the groups (**figure 20b**). In the earlier time points, the treated wound actually expanded, but started contracting at day 7 and

eventually caught up with the control group. The contraction was followed by wound expansion at later time points, possibly due to the subject's general growth in body mass.

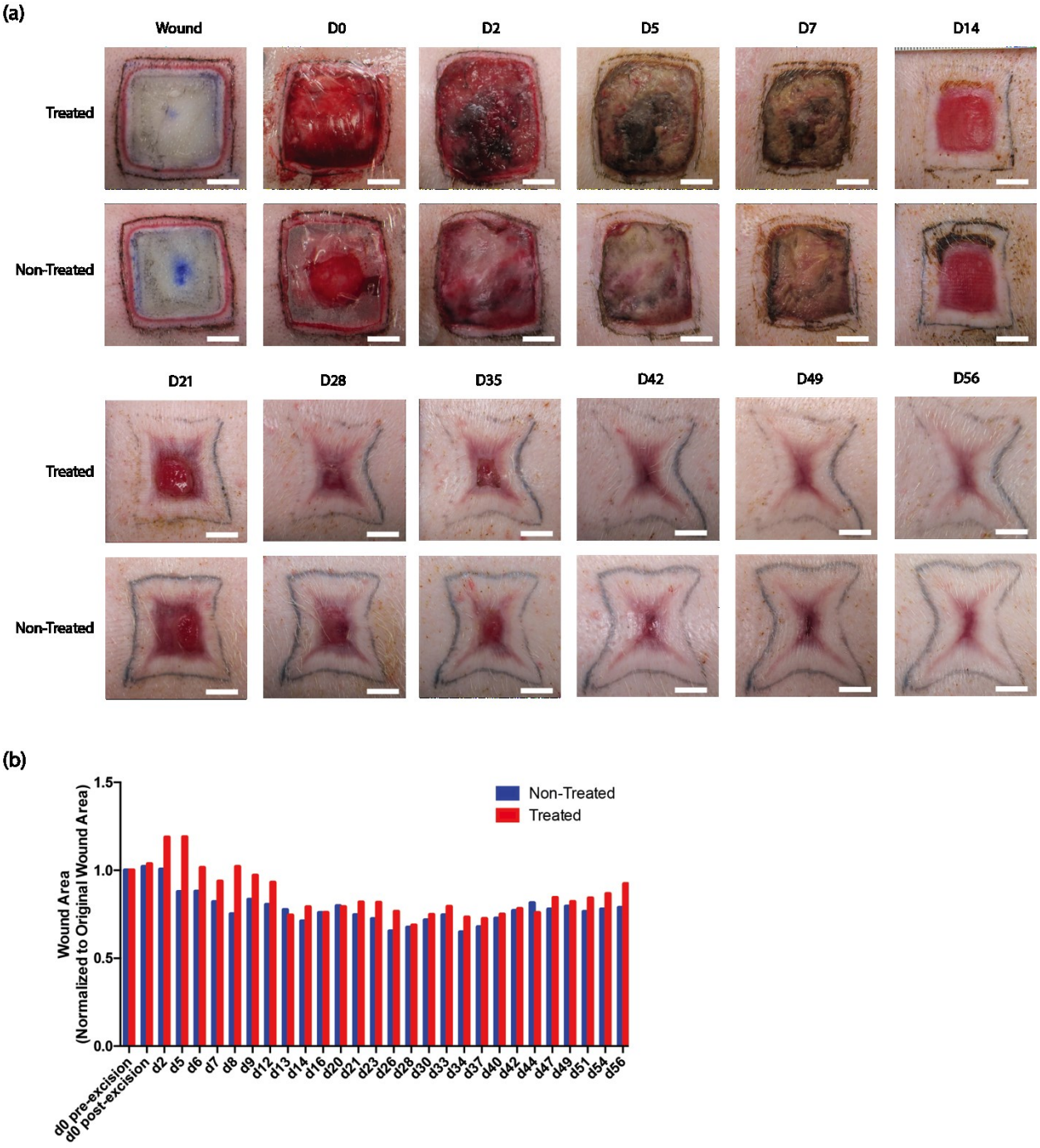

Figure 20. Macroscopic view of healing wounds and contraction. (a) Macroscopic view of healing wounds (3cm x 3cm). (Bar = 1cm) (b) Quantification of the area inside the tattooed edges of each wound.

Discussion

In general, porcine model showed a different response to the Dex-AE/PEGDA hydrogel compared to the murine model. This could be due to the procedural difference or the physiological difference between the two models that were exploited. For example, the hydrogel was degraded almost completely by day 5, whereas in murine model, the complete degradation of the hydrogel took more than a week [21]. One possible explanation could be that the inflammatory cells in pigs infiltrate and degrade the gels much faster than those in mice. Fast degradation could also be due to possible bacterial infection in the early stage of the wound healing. The hydrogel degradation can be accelerated with the addition of bacteria since these cells are able to degrade dextran with a variety of endo- and exo-dextranases [34]. The dark discoloration of the wounds in days 2 and 5 that seems like a necrotic tissue may also be due to the possible infection.

We observed higher blood flow and higher vessel coverage around the wound edges at day 5, but we could not observe further significant differences in the vascularization process between the two groups after that time point. We did however observe better thinning of the epithelial layer after the re-epithelialization and also observed bigger blood vessels near the epithelial layer at day 7. Better blood flow to the epithelium at the early time point could have contributed to better epithelial healing.

In terms of re-epithelialization, we learned that the pigs scratch their backs often during the first three weeks of treatment where the wounds were created. Sometimes this resulted in re-opening of the wounds, confirmed by increased blood flow measurement at these time points. There are ways to numb their backs and prevent them from scratching,

but these methods are invasive and may interfere with the healing process. The better way would be to use additional dressing above the wounds to minimize the physical damaging of the wounds by the scratching.

qPCR data at day 14 give interesting perspective on wound healing in terms of gene expression profiles, but more data at different time points are needed to observe the change in these profiles over time in order to make an informed conclusion.

Addition studies need to be conducted to optimize the treatment protocol, to strengthen statistical significance, and to investigate the effect of removing the peripheral wound on small wound healing. Removing the peripheral wound completely before the hydrogel treatment seems to enhance cellular infiltration of the hydrogel for the bigger wounds. This may enhance and expedite the healing process for the treated groups. We also need to repeat the big wound study with more time points for histological assessment to monitor the healing progress at the microscopic level. In addition, wound contraction data needs to be normalized by the pig's body growth. This may be achieved by tattooing the area near the wound that does not contract with the wound and measure the increase in the body surface area.

There may be other ways to design the hydrogel to enhance the healing process. For example, cell attachment sites such as RGD amino acid sequence can be added to the hydrogel so the host cells can migrate into the hydrogel better. However, the hydrogel should be designed to be degraded slower so the attachment sites stay intact while the cells migrate. The hydrogel can also be loaded with growth factors such as VEGF and EGF, which may enhance the cellular response to the treatment. However, adding

biological factors is not practical since this would result in the hydrogel going through tougher FDA restrictions and delaying the use in clinical settings. Therefore, before changing the designs of the Dex-AE/PEGDA hydrogel, we need to perform additional experiments as described above to ascertain the therapeutic effects of the hydrogel.

Conclusion

Preliminary data suggest a higher blood supply in the hydrogel-treated wounds that may have contributed to the better epithelial healing that we observed in the treated wounds. The Dex-AE/PEGDA hydrogels degrade within 5 days after their implantation, and more infiltrated cells were observed in the treated group with fully excised wounds compared to the treated group with partially excised wounds and non-treated group. More studies with wounds with full-excision need to be done in order to investigate the therapeutic effect of the hydrogel and understand the change in expression levels of wound healing genes over a longer period of time for both treated and non-treated groups. Moreover, additional studies involving bigger wounds need to be performed to give statistical significance to the enhanced vasculature that we observed in this study.

Bibliography

[1] Singer AJ, McClain SA. A Porcine Burn Model. Wound Healing: Methods and Protocols2003. p. 107-19.
[2] National Burn Repository Annual Report 2014: American Burn Association; 2014.
[3] Sheridan RL. Burns : a practical approach to immediate treatment and long-term care. London :: Manson Publishing; 2012.
[4] Myers BA. Wound management : principles and practice. 2nd ed. ed. Upper Saddle Rover, N.J. :: Pearson/Prentice Hall; 2008.
[5] Falabella A. Wound Healing. In: Kirsner R, editor. Hoboken :: Taylor and Francis; 2013.
[6] Tonnesen MG, Feng X, Clark RA. Angiogenesis in wound healing. Journal of Investigative Dermatology symposium proceedings: Nature Publishing Group; 2000. p. 40-6.
[7] Brown LF, Yeo K, Berse B, Yeo T-K, Senger DR, Dvorak HF, et al. Expression of vascular permeability factor (vascular endothelial growth factor) by epidermal keratinocytes during wound healing. The Journal of experimental medicine. 1992;176:1375-9.
[8] Nissen NN, Polverini P, Koch AE, Volin MV, Gamelli RL, DiPietro LA. Vascular endothelial growth factor mediates angiogenic activity during the proliferative phase of wound healing. The American journal of pathology. 1998;152:1445.
[9] Clark R, Tonnesen MG, Gailit J, Cheresh DA. Transient functional expression of alphaVbeta 3 on vascular cells during wound repair. The American journal of pathology. 1996;148:1407.
[10] Supp DM. Skin substitutes for burn wound healing: current and future approaches. 2011.
[11] Middelkoop E, van den Bogaerdt AJ, Lamme EN, Hoekstra MJ, Brandsma K, Ulrich MMW. Porcine wound models for skin substitution and burn treatment. Biomaterials. 2004;25:1559-67.
[12] Sullivan TP, Eaglstein WH, Davis SC, Mertz P. The pig as a model for human wound healing. Wound repair and regeneration. 2001;9:66-76.
[13] Drury JL, Mooney DJ. Hydrogels for tissue engineering: scaffold design variables and applications. Biomaterials. 2003;24:4337-51.
[14] Hoffman AS. Hydrogels for biomedical applications. Advanced Drug Delivery Reviews. 2012;64:18-23.
[15] Peppas NA, Hilt JZ, Khademhosseini A, Langer R. Hydrogels in biology and medicine: from molecular principles to bionanotechnology. Advanced materials. 2006;18:1345-60.
[16] Burdick JA, Prestwich GD. Hyaluronic acid hydrogels for biomedical applications. Advanced materials. 2011;23:H41-H56.
[17] Loessner D, Rizzi SC, Stok KS, Fuehrmann T, Hollier B, Magdolen V, et al. A bioengineered 3D ovarian cancer model for the assessment of peptidase-mediated enhancement of spheroid growth and intraperitoneal spread. Biomaterials. 2013;34:7389-400.

[18] Weis SM, Cheresh DA. Tumor angiogenesis: molecular pathways and therapeutic targets. Nature medicine. 2011;17:1359-70.
[19] Sun G, Shen YI, Ho CC, Kusuma S, Gerecht S. Functional groups affect physical and biological properties of dextran-based hydrogels. Journal of biomedical materials research Part A. 2010;93:1080-90.
[20] Sun G, Shen YI, Kusuma S, Fox-Talbot K, Steenbergen CJ, Gerecht S. Functional neovascularization of biodegradable dextran hydrogels with multiple angiogenic growth factors. Biomaterials. 2011;32:95-106.
[21] Sun G, Zhang X, Shen Y-I, Sebastian R, Dickinson LE, Fox-Talbot K, et al. Dextran hydrogel scaffolds enhance angiogenic responses and promote complete skin regeneration during burn wound healing. Proceedings of the National Academy of Sciences. 2011;108:20976-81.
[22] Sun G, Chu C-C. Synthesis, characterization of biodegradable dextran–allyl isocyanate–ethylamine/polyethylene glycol–diacrylate hydrogels and their in vitro release of albumin. Carbohydrate Polymers. 2006;65:273-87.
[23] Zhang X, Wei X, Liu L, et al. ASsociation of increasing burn severity in mice with delayed mobilization of circulating angiogenic cells. Archives of Surgery. 2010;145:259-66.
[24] Kusuma S, Zhao S, Gerecht S. The extracellular matrix is a novel attribute of endothelial progenitors and of hypoxic mature endothelial cells. The FASEB Journal. 2012;26:4925-36.
[25] Singh A, Elisseeff J. Biomaterials for stem cell differentiation. Journal of Materials Chemistry. 2010;20:8832-47.
[26] Branski LK, Mittermayr R, Herndon DN, Norbury WB, Masters OE, Hofmann M, et al. A porcine model of full-thickness burn, excision and skin autografting. Burns : journal of the International Society for Burn Injuries. 2008;34:1119-27.
[27] Robson MC. Physiological Responses to Burning Injury. JAMA. 1983;249:3252-.
[28] Gaines C, Poranki D, Du W, Clark RA, Van Dyke M. Development of a porcine deep partial thickness burn model. Burns : journal of the International Society for Burn Injuries. 2013;39:311-9.
[29] Papp A, Kiraly K, Härmä M, Lahtinen T, Uusaro A, Alhava E. The progression of burn depth in experimental burns: a histological and methodological study. Burns : journal of the International Society for Burn Injuries. 2004;30:684-90.
[30] Ebrahimian TG, Squiban C, Roque T, Lugo‐Martinez H, Hneino M, Buard V, et al. Plasminogen Activator Inhibitor‐1 Controls Bone Marrow‐Derived Cells Therapeutic Effect Through MMP9 Signaling: Role in Physiological and Pathological Wound Healing. Stem Cells. 2012;30:1436-46.
[31] Salo T, Mäkelä M, Kylmäniemi M, Autio-Harmainen H, Larjava H. Expression of matrix metalloproteinase-2 and-9 during early human wound healing. Laboratory investigation; a journal of technical methods and pathology. 1994;70:176-82.
[32] Marikovsky M, Breuing K, Liu PY, Eriksson E, Higashiyama S, Farber P, et al. Appearance of heparin-binding EGF-like growth factor in wound fluid as a response to injury. Proceedings of the National Academy of Sciences. 1993;90:3889-93.

[33] Tolino MA, Block ER, Klarlund JK. Brief treatment with heparin-binding EGF-like growth factor, but not with EGF, is sufficient to accelerate epithelial wound healing. Biochimica et Biophysica Acta (BBA)-General Subjects. 2011;1810:875-8.
[34] Khalikova E, Susi P, Korpela T. Microbial dextran-hydrolyzing enzymes: fundamentals and applications. Microbiology and Molecular Biology Reviews. 2005;69:306-25.

GRECO SONG

2923 Saint Paul St. APT 1, Baltimore MD 21218 | 714-300-3697 | grecosong@gmail.com

EDUCATION

MIT-Harvard Division of Health Sciences and Technology
Ph.D. in Medical Engineering and Medical Physics **2020**

Johns Hopkins University
M.S.E. in Chemical and Biomolecular Engineering **2014**
Thesis: "A Dextran-Allyl Isocyanate-Ethylamine Hydrogel For Treating Third-Degree Dermal Burn Wounds"

Johns Hopkins University
B.S. in Chemical and Biomolecular Engineering **2013**
Molecular and Cellular Bioengineering Concentration
General Honors and Departmental Honors

AWARDS

Dean's List 2009 – 2013

RELATED EXPERIENCE

Gerecht Lab
Graduate Researcher **2013 – 2014**

- Applying dextran-based hydrogels to the treatment of burn wounds in *in vivo* murine and porcine models.
- Modeling tumor angiogenesis in a 3D *in vitro* environment using hypoxia-inducing gelatin hydrogel.

Gerecht Lab
Undergraduate Research Assistant **2012 – 2013**

- Synthesis and characterization of allyl- and ethylamine-modified dextran polymers.
- Modeling tumor microenvironment *in vitro* with RGD/MMP-modified hyaluronic acid hydrogels.

Laboratory for Craniofacial & Orthopaedic Tissue Engineering
Undergraduate Laboratory Asistant **2010 – 2011**

- Three-dimensional modeling of osteonecrosis *in vitro* using mesenchymal stem cells and understanding the effect of glucocorticoid on bone vasculature.
- Optimizing a protocol for bone-graft integration using torsional mechanical testing

PUBLICATIONS AND CONFERENCES

1. **Song HG,** Park KM, Gerecht S. "Hydrogels for Three-Dimensional Modeling of Tumor Angiogenesis." *Advanced Drug Delivery Reviews*, accepted.
2. Shen YI, **Song HG**, Sun G, Hanjaya-Putra D, Gerecht S. "Engineering Bioactive Hydrogels for Treating Full Thickness Dermal Wounds." AIChE: 2013 Annual Meeting. San Francisco, CA. Nov 3-8, 2013. Oral presentation.

MEMBERSHIPS

Tau Beta Pi Engineering Honors Society
Vocal Chords A Cappella